SPANDIDOS PUBLICATIONS

ONCOLOGY LETTERS 19: 3799-3814, 2020

Identification of differentially expressed genes and biological pathways in para-carcinoma tissues of HCC with different metastatic potentials

YAN LIU[1*], MINGMING DENG[2*], YIMENG WANG[1], HUIQIN WANG[1], CHANGPING LI[2] and HAO WU[3]

[1]Department of Gastroenterology, The Chengdu Fifth People's Hospital, Chengdu, Sichuan 611130; [2]Department of Gastroenterology, The Affiliated Hospital of Southwest Medical University, Luzhou, Sichuan 646000; [3]Department of Hepatobiliary Surgery, The Second Affiliated Hospital of Chongqing Medical University, Chongqing 400016, P.R. China

Received July 22, 2019; Accepted January 30, 2020

DOI: 10.3892/ol.2020.11493

Abstract. Hepatocellular carcinoma (HCC) is a malignant tumor with extensive metastasis. Changes in the tumor microenvironment provide favorable conditions for tumor metastasis. However, the role of changes to the tumor microenvironment in HCC metastasis is yet to be elucidated. The Gene Expression Omnibus expression profile GSE5093 consists of 20 noncancerous tissues surrounding HCC tissues, including 9 metastasis-inclined microenvironment samples with detectable metastases and 11 metastasis-averse microenvironment samples without detectable metastases. The present study assessed 35 HCC samples to verify the results of chip analysis. In total, 712 upregulated and 459 downregulated genes were identified, with 1,033 nodes, 7,589 edges and 10 hub genes. Gene ontology and Kyoto Encyclopedia of Genes and Genomes pathway analysis revealed that the differentially expressed genes were significantly enriched in 'cell-cell adhesion', 'cell proliferation' and 'protein binding'. The top 10 hub genes were identified via a protein-protein interaction analysis. The 3 most significant modules were identified from the protein-protein network. Moreover, an association between hub genes and patient prognosis was identified. In conclusion, these candidate genes and pathways may help elucidate the mechanisms underlying HCC metastasis and identify more options for targeted therapy.

Correspondence to: Dr Changping Li, Department of Gastroenterology, The Affiliated Hospital of Southwest Medical University, 25 Taiping Street, Luzhou, Sichuan 646000, P.R. China
E-mail: 506854209@qq.com

Dr Hao Wu, Department of Hepatobiliary Surgery, The Second Affiliated Hospital of Chongqing Medical University, 76 Linjiang Road, Chongqing 400016, P.R. China
E-mail: whwhcq@126.com

*Contributed equally

Key words: hepatocellular carcinoma, tumor microenvironment, differentially expressed genes, enrichment analysis, protein-protein interaction, prognosis

Introduction

Hepatocellular carcinoma (HCC) is the major histological subtype of primary liver cancer accounting for 85% of all liver cancer cases worldwide, and it was reported to be the most common liver malignancy in 2016 (1). HCC is one of the most aggressive types of cancer with a high mortality rate, whereby 326,000 people died of HCC in 2015 (2). There are several definite risk factors for HCC, such as chronic hepatitis B/C virus infection, nonalcoholic fatty liver diseases, aflatoxin consumption and smoking (2). In addition, there have been a number of identified prognostic markers of HCC, such as alpha fetoprotein, vascular endothelial growth factor and transforming growth factor β, in both large-scale clinical trials and research projects. However, the early diagnosis and effective treatment of HCC remains problematic (3).

To date, surgical resection remains the gold standard treatment for HCC; however, postoperative recurrence and metastasis is common (4). In addition, a large number of patients with HCC are diagnosed at the advanced stages, in which the tumor has already metastasized to other organs prior to surgery (4). Therefore, metastasis is a key challenge in the treatment of HCC. Tumor metastasis is a malignant biological process involving multiple factors and complex signaling pathways that depend not only on the genetic changes of malignant tumor cells, but also on the changes in the tumor microenvironment, such as the stroma, blood vessels and infiltrating inflammatory cells (5). Dysfunction of gene expression in the microenvironment surrounding a tumor serves an important role in the metastatic behavior of tumor cells, such as adhesion of tumor cells, degradation of the extracellular matrix, invasion of basal tissues, homing ability to enter specific tissues, movement and migration in the circulatory system and the promotion of the angiogenesis (6). Therefore, the identification of key genes which function in the tumor microenvironment

of HCC may be helpful to identify new targeted therapeutic strategies for HCC metastasis.

In the present study, an original dataset (GSE5093) was obtained from the NCBI-Gene Expression Omnibus database (ncbi.nlm.nih.gov/geo/) containing 20 samples of noncancerous tissues surrounding HCC tissues from two distinct groups of patients with HCC, including 9 metastasis-inclined microenvironment (MIM) samples, with detectable metastases and 11 metastasis-averse microenvironment (MAM) samples, without detectable metastases (7). Differentially expressed genes (DEGs) were filtered in using the Morpheus Website with a data processing standard. Gene-Spring software (version 13.1.1; Agilent Technologies Inc.) was employed to screen the DEGs, followed by Gene Ontology (GO) and Kyoto Encyclopedia of Genes and Genomes (KEGG; kegg.jp) pathway enrichment analysis. Furthermore, a protein-protein interaction (PPI) network was established and three significant modules were analyzed. A total of 35 HCC tissue samples were assessed to verify the results of chip analysis. The present study aimed to investigate the genetic molecular mechanisms underlying the metastatic phenotype of HCC and improve the diagnosis and treatment of metastases of primary hepatic carcinoma patients.

Materials and methods

Data collection. The gene expression profile GSE5093 was obtained from Gene Expression Omnibus (GEO) (7). The GSE5093 dataset was based on the GPL1262 dataset [National Cancer Institute (NCI)/Advanced Technology Corner (ATC) Hs-UniGEM2, Advanced Technology Center Microarray Facility (National Institutes of Health (NIH)/NCI/Cancer Research Center (CCR)/ATC)] and contained 20 samples, including 9 MIM samples and 11 MAM samples.

Patients and specimens. The present study was approved by The Institutional Review Board of the Second Affiliated Hospital of Chongqing Medical University (Chongqing, China) and written informed consent was provided by all patients according to The Declaration of Helsinki. A total of 35 HCC specimens (from 21 men and 14 women; age range, 22-73 years; mean age, 53 years) were collected during resection of HCC tumor at The Second Affiliated Hospital of Chongqing Medical University (Chongqing, China) between May 2015 and November 2016. Tissue samples included 16 noncancerous surrounding hepatic tissue samples with MIM and 19 noncancerous surrounding hepatic tissue samples with MAM (<5 cm away from HCC tissue). Specimens were stored in liquid nitrogen for subsequent experimentation. The clinicopathological features of the HCC specimens are listed in Table SI.

Identification and analysis of DEGs. MIM and MAM samples were divided into two groups and GEO2R (ncbi.nlm.nih.gov/geo/geo2r/) was used to analyze the DEGs between the two groups. The raw expression data files, which included TXT files (Agilent platform), were used for analysis by processing using the Morpheus Website (software.broadinstitute.org). A unpaired t-test was used to identify the DEGs and |log fold change (FC)|≥1 and P<0.05 were used as the cut-off criteria for statistical significance.

Functional and pathway enrichment of DEGs. After identifying the DEGs, GO enrichment and KEGG pathway analyses were performed for gene annotation and functional enrichment analysis using the online tool Database for Annotation, Visualization and Integrated Discovery (DAVID; david.abcc.ncifcrf.gov/). The resulting GO terms and KEGG pathways with P<0.05 were considered significantly enriched for the obtained DEGs.

Survival analysis of the hub genes in HCC. Kaplan-Meier survival analysis and the log-rank test were employed to determine the association between hub genes and HCC, using the Gene Expression Profiling Interactive Analysis (GEPIA) database (8) and prognostic data from The Cancer Genome Atlas (cancer.gov/tcga) database. The percentage of low and high expression groups was set at 50%.

Constructing the PPI network of DEGs. The Search Tool for the Retrieval of Interacting Genes (STRING) database offers both experimental and predicted interactive information (9). In the present study, the STRING database was used to explore the enrichment analysis results according to the biological process, molecular function and cell components determined for the DEGs. Finally, the interactions were selected, of which combined scores of >0.7 were used to construct the PPI network using the Molecular Complex Detection (MCODE) plugin within Cytoscape software [version 3.7.2; (10,11)].

RNA preparation and reverse transcription-quantitative (RT-q)PCR. Total RNA from tissue samples was extracted using TRIzol® reagent (Takara Bio, Inc.), according to the manufacturer's protocol. RNA was reverse transcribed into cDNA using the PrimeScript RT reagent (Takara Bio, Inc.). The temperature protocol for RT was as follows: 37˚C for 5 min, followed by 45˚C for 42 min and 75˚C for 5 min. qPCR was subsequently performed using SYBR-Green Real-time PCR Master mix (Beijing Transgen Biotech Co., Ltd.). The primer sequences used for qPCR are listed in Table SII. The following thermocycling conditions were used for qPCR: Initial denaturation at 92˚C for 15 min; 37 cycles of 95˚C for 15 sec, 55˚C for 30 sec; and a final extension at 72˚C for 30 sec. Relative mRNA levels were measured using the $2^{-\Delta\Delta Cq}$ method (12) and normalized to the internal reference gene GAPDH.

Statistical analysis. All data are presented as the mean ± standard deviation and analyzed using SPSS 20.0 software (IBM Corp.) and GraphPad Prism 7 (GraphPad Software, Inc.). Differences between groups were analyzed using paired Student's t-test and one-way analysis of variance, followed by Newman-Keuls post hoc test. P<0.05 was considered to indicate a statistically significant difference.

Results

Identification of DEGs between MIM and MAM samples. Through the analysis and processing of data in GSE5093, a total of 1,171 DEGs were identified, which included 712 upregulated and 459 downregulated genes. The heat map of DEG expression levels (top 50 upregulated and 50 downregulated genes) is exhibited in (Fig. 1).

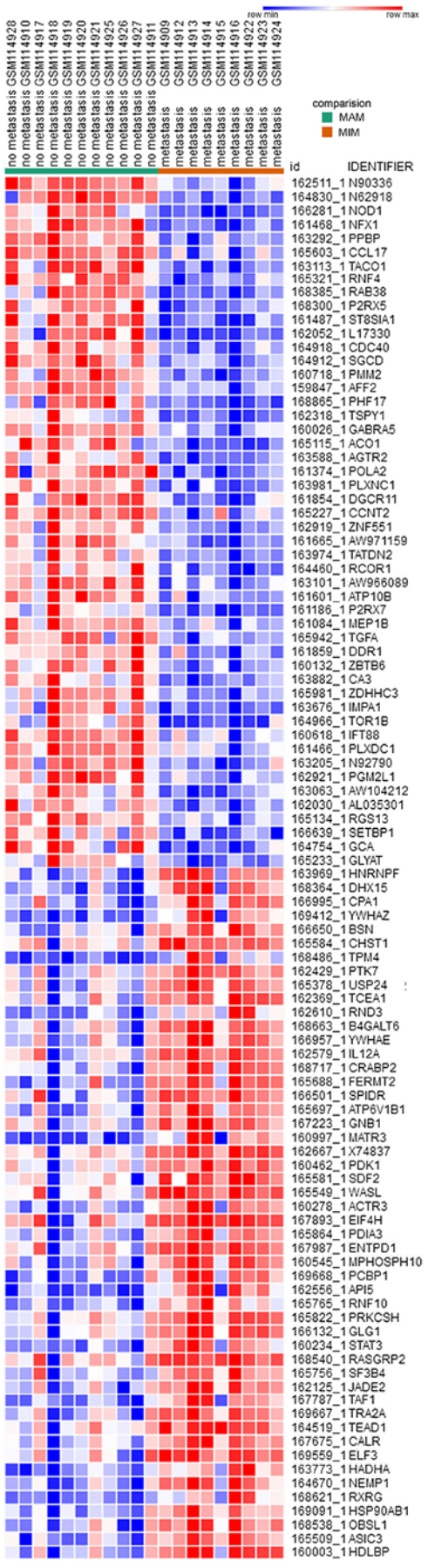

Figure 1. Heat map of the top 100 differentially expressed genes in metastasis-inclined microenvironment and metastasis-averse microenvironment samples (50 upregulated and 50 downregulated genes). Red, upregulation; blue, downregulation.

GO and pathway enrichment analyses of DEGs. The 1,171 DEGs were selected for functional analysis, performed using the DAVID database. GO analysis of DEGs was carried out from three aspects, which covered molecular function (MF), cellular component (CC) and biological process (BP). BP analysis revealed that the upregulated DEGs were enriched in 'cell-cell adhesion', 'mRNA splicing via spliceosome' and 'platelet degranulation' (Table I), whereas the downregulated DEGs were enriched in 'cell-cell adhesion', 'cell proliferation' and 'positive regulation to tyrosine phosphorylation of STAT5 protein' (Table II). For CC, the upregulated DEGs were enriched in the 'extracellular exosome and cytosol', as well as the 'membrane' (Table I) and the downregulated DEGs were enriched in 'receptor complex', 'integral component of plasma membrane' and 'postsynaptic density' (Table II). In addition, the MF of upregulated DEGs were enriched in 'protein binding', 'poly(A) RNA binding' and 'cadherin binding involved in cell-cell adhesion' (Table I), whereas the downregulated DEGs were enriched in 'protein binding', 'epidermal growth factor receptor binding' and 'amino acid transmembrane transfer activity' (Table II). These results suggest that the DEGs were associated with the biological processes of cell migration and metastasis.

KEGG pathway analysis of MIM and MAM DEGs. To further analysis the functions of DEGs, KEGG pathway analysis was conducted to determine the most significantly enriched pathways of the upregulated DEGs and downregulated DEGs. The upregulated DEGs were enriched in 'protein processing in the endoplasmic reticulum', 'antigen processing and presentation' and 'phagosome' pathways (Table III). The downregulated DEGs were enriched in the 'arrhythmogenic right ventricular cardiomyopathy', 'phosphatidylinositol signaling system' and 'inositol phosphate metabolism' pathways (Table III).

Analysis of the PPI network with DEGs in MIM and MAM. According to the information provided by the STRING, the interaction of the DEGs and acquired hub genes of potential diagnosis and treatment associated DEGs were analyzed. As depicted in Figs. 2A and S1, there were 955 nodes and 7,589 edges, of which 638 nodes represented upregulated DEGs and nodes represented downregulated DEGs (Fig. 2B). The top 10 hub genes with the highest degrees included: Heat shock protein family A member 8 (HSPA8); PH domain and leucine rich repeat protein phosphatase 1 (PHLPP1); phosphoribosylglycinamide formyltransferase (GART); carbamoyl-phosphate synthetase 2 (CAD); actin beta (ACTB); cadherin 1 (CDH1); phosphatidylinositol-4,5-bisphosphate 3-kinase catalytic subunit γ (PIK3CG); nuclear factor κB subunit 1 (NFκB1); signal transducer and activator of transcription 3 (STAT3); and heat shock protein family A (Hsp70) member 5 (HSPA5). Then, the expression of the top 10 hub genes were verified using RT-qPCR. There were 4 hub upregulated genes and 6 downregulated genes in MAM, compared with MIM samples (Fig. 3). Moreover, the top 3 significant modules were selected from the DEG PPI network using MCODE (Fig. 4A-C). Module 1 included 31 nodes and 458 edges, module 2 included 37 nodes and 267 edges and module 3 included 45 nodes. Furthermore,

Table I. Gene ontology analysis of upregulated differentially expressed genes associated with metastasis-inclined microenvironment and metastasis-averse microenvironment.

Category	Term	Gene function	Gene count	P-value
BP	GO:0098609	Cell-cell adhesion	37	2.9×10^{-10}
BP	GO:0000398	mRNA splicing, via spliceosome	28	3.1×10^{-7}
BP	GO:0002576	Platelet degranulation	18	7.1×10^{-7}
BP	GO:0006457	Protein folding	22	1.2×10^{-5}
BP	GO:0048013	Ephrin receptor signaling pathway	14	3.8×10^{-5}
BP	GO:0043066	Movement of cell or subcellular component	14	3.8×10^{-5}
BP	GO:0043066	Negative regulation of apoptotic process	38	4.2×10^{-5}
BP	GO:0007165	Signal transduction	75	5.4×10^{-5}
BP	GO:0019886	Antigen processing and presentation of exogenous peptide antigen via MHC class II	14	7.8×10^{-5}
BP	GO:0050900	Leukocyte migration	16	1.1×10^{-4}
CC	GO:0070062	Extracellular exosome	220	1.1×10^{-28}
CC	GO:0016020	Membrane	170	7.6×10^{-21}
CC	GO:0005829	Cytosol	218	1.4×10^{-18}
CC	GO:0005654	Nucleoplasm	177	4.2×10^{-13}
CC	GO:0005913	Cell-cell adherens junction	44	5.2×10^{-13}
CC	GO:0031012	Extracellular matrix	37	5.5×10^{-10}
CC	GO:0042470	Melanosome	21	9.2×10^{-10}
CC	GO:0043209	Myelin sheath	25	2.5×10^{-9}
CC	GO:0005615	Extracellular space	90	1.1×10^{-7}
CC	GO:0030529	Intracellular ribonucleoprotein complex	21	1.8×10^{-7}
MF	GO:0005515	Protein binding	448	2.8×10^{-14}
MF	GO:0044822	Poly(A) RNA binding	100	7.6×10^{-14}
MF	GO:0098641	Cadherin binding involved in cell-cell adhesion	42	1.8×10^{-12}
MF	GO:0032403	Protein complex binding	23	2.8×10^{-5}
MF	GO:0003723	RNA binding	43	4.3×10^{-5}
MF	GO:0051287	NAD binding	9	1.1×10^{-4}
MF	GO:0051082	Unfolded protein binding	15	1.3×10^{-4}
MF	GO:0008134	Transcription factor binding	25	4.8×10^{-4}
MF	GO:0005524	ATP binding	86	5.9×10^{-4}
MF	GO:0019899	Enzyme binding	27	9.6×10^{-4}

P<0.001. GO, Gene Ontology; BP, biological process; CC, cellular component; MF, molecular function.

GO and KEGG pathway analysis results were used to analyze the functional and signal pathway enrichment of the three modules. The results showed that module 1 was primarily associated with 'RNA splicing', 'catalytic step 2 spliceosome', 'nucleotide binding' and 'spliceosome' pathways (Table IV). Module 2 was primarily enriched in 'protein modification by small protein conjugation', 'catalytic complex', 'ubiquitin-protein transferase activity' and 'chemokine signaling' pathways (Table V). Module 3 was most enriched in 'protein folding', 'extracellular exosomes', 'protein disulfide isomerase activity' and 'chemokine signaling' pathways (Table VI). These results indicated that the 10 hub genes may function in the biological behavior processes of cell migration and metastasis.

The Kaplan-Meier plot of hub genes in MIM and MAM. Through GEPIA prediction of the association between the 10 hub genes and HCC patient prognosis, it was observed that expression of CAD [Hazard Ratio (HR), 1.9; P<0.001], GART (HR, 1.8; P=0.018), HSPA5 (HR, 1.5; P=0.016), ACTB (HR, 1.6; P=0.0074), CDH1 (HR, 0.66; P=0.018) and HSPA8 (HR, 1.6; P=0.011) were associated with poor overall survival in patients with HCC (Fig. 5).

Discussion

HCC is the most common malignant tumor with high morbidity and mortality, and was reported to be one of the major causes of cancer-associated mortalities worldwide, in 2002 (13). Patients with HCC are often diagnosed with extrahepatic metastasis, which poses a great challenge to the diagnosis and treatment of HCC (14). Currently, high-throughput gene chip technology can be used to explore the occurrence and development of diseases from the whole genome or transcriptome

Table II. Gene ontology analysis of downregulated differentially expressed genes associated with metastasis-inclined microenvironment and metastasis-averse microenvironment.

Category	Term	Gene function	Gene count	P-value
BP	GO:0007155	Cell adhesion	28	$^{c}2.8x10^{-5}$
BP	GO:0008283	Cell proliferation	22	$^{c}3.0x10^{-4}$
BP	GO:0042523	Positive regulation of tyrosine phosphorylation of Stat5 protein	5	$^{c}6.7x10^{-4}$
BP	GO:0007165	Signal transduction	47	$^{c}9.4x10^{-4}$
BP	GO:0031532	Actin cytoskeleton reorganization	6	$^{b}5.8x10^{-3}$
BP	GO:0009267	Cellular response to starvation	6	$^{b}5.8x10^{-3}$
BP	GO:0060749	Mammary gland alveolus development	4	$^{b}7.8x10^{-3}$
BP	GO:0007169	Transmembrane receptor protein tyrosine kinase signaling pathway	8	$^{b}9.5x10^{-3}$
BP	GO:0006865	Amino acid transport	5	$^{b}1.0x10^{-2}$
BP	GO:0045944	Positive regulation of transcription from RNA polymerase II promoter	37	$^{a}1.1x10^{-2}$
CC	GO:0043235	Receptor complex	90	$^{c}1.9x10^{-4}$
CC	GO:0005887	Integral component of plasma membrane	47	$^{c}4.1x10^{-4}$
CC	GO:0014069	Postsynaptic density	78	$^{b}1.3x10^{-3}$
CC	GO:0045211	Postsynaptic membrane	64	$^{b}1.4x10^{-3}$
CC	GO:0005829	Cytosol	52	$^{b}2.1x10^{-3}$
CC	GO:0005886	Plasma membrane	52	$^{b}3.6x10^{-3}$
CC	GO:0009986	Cell surface	52	$^{b}4.5x10^{-3}$
CC	GO:0030054	Cell junction	15	$^{b}5.8x10^{-3}$
CC	GO:0005794	Golgi apparatus	8	$^{b}6.7x10^{-3}$
CC	GO:0005737	Cytoplasm	8	$^{b}7.5x10^{-3}$
MF	GO:0005515	Protein binding	258	$^{c}1.5x10^{-5}$
MF	GO:0005154	Epidermal growth factor receptor binding	6	$^{c}8.6x10^{-4}$
MF	GO:0015171	Amino acid transmembrane transporter activity	7	$^{c}8.6x10^{-4}$
MF	GO:0005524	ATP binding	56	$^{c}9.5x10^{-4}$
MF	GO:0042803	Protein homodimerization activity	32	$^{b}1.5x10^{-3}$
MF	GO:0004714	Transmembrane receptor protein tyrosine kinase activity	6	$^{b}2.1x10^{-3}$
MF	GO:0008179	Adenylate cyclase binding	3	$^{a}1.9x10^{-2}$
MF	GO:0001078	Transcriptional repressor activity, RNA polymerase II core promoter proximal region sequence-specific binding	8	$^{a}1.9x10^{-2}$
MF	GO:0005096	Gtpase activator activity	14	$^{a}2.0x10^{-2}$
MF	GO:0043236	Laminin binding promoter	4	$^{a}2.2x10^{-2}$

$^{a}P<0.05$, $^{b}P<0.01$, $^{c}P<0.001$. GO, Gene Ontology; BP, biological process; CC, cellular component; MF, molecular function.

level, which has been widely used in gene expression analysis and biomarker discovery for a variety of illnesses (14). In order to further understand the molecular mechanisms underlying the recurrence and metastasis of HCC, the GSE5093 Biochip dataset on the metastatic microenvironment of HCC was obtained from the GEO database. This was used to perform a systematic and bioinformatics analysis, including enrichment analysis of differences in gene expression and protein-protein interaction.

In the present study, a total of 1,171 DEGs were identified, of which 712 were upregulated and 459 were downregulated. GO term functional analysis demonstrated that the upregulated genes were primarily involved in 'cell-cell adhesion', 'extracellular exosome' and 'cadherin binding', while downregulated DEGs were involved in 'cell-cell adhesion', 'integral component of plasma membrane' and 'epidermal growth factor receptor binding'. The tumor cells leave the primary site, invade the extracellular matrix, adhere to macromolecular protein components in the basement membrane, degrade the basement membrane and the extracellular matrix, and move through the extracellular matrix to invade the surrounding tissues (15). Once in the circulation system, tumor cells evade the surveillance of the immune system. When passing through the vessel wall to

Table III. Kyoto Encyclopedia of Genes and Genomes pathway analysis of DEGs associated with metastasis-inclined microenvironment and metastasis-averse microenvironment.

A, Upregulated DEGs

Pathway	Name	Gene count	P-value	Genes
hsa04141	Protein processing in endoplasmic reticulum	26	[c]7.50×10^{-6}	HSP90AB1, SEC31A, GANAB, PDIA3, PDIA4, PRKCSH, CALR, SEC62, DERL3, CANX, SSR1, OS9, HSPH1,xBP1, RPN1, DNAJA1, HSPA6, HSPA5, HSPA8, SEC23A, P4HB, BCAP31, CAPN1, SEC23B, SEL1L, UBE2E1
hsa04612	Antigen processing and presentation	15	[c]7.23×10^{-5}	HSP90AB1, CIITA, PDIA3, CD8B, LGMN, CTSS, CALR, CANX, TAPBP, HSPA6, HLA-DRB5, CTSB, HLA-DPB1, HSPA8, HLA-DRA
hsa04145	Phagosome	22	[c]9.24×10^{-5}	ACTB, C3, ATP6AP1, CTSS, CALR, ATP6V1B1, ITGB1, CANX, ITGAM, ACTG1, ATP6V1A, LAMP2, HLA-DRB5, MPO, VAMP3, HLA-DPB1, THBS1, FCGR3A, DYNC1H1, THBS2, CD14, HLA-DRA
hsa03040	Spliceosome	20	[c]1.51×10^{-4}	SRSF1, TRA2A, PRPF3, DDX5, SF3A1, SF3B4, RBMX, HNRNPA1, HNRNPU, SRSF4, HNRNPK, PLRG1, DHX38, PCBP1, USP39, HSPA6, DHX15, ACIN1, HSPA8, THOC1
hsa04918	Thyroid hormone synthesis	13	[c]4.73×10^{-4}	TG, GPX2, ADCY7, GNAQ, ATP1B2, PAX8, TPO, CREB3L1, PRKCG, PRKACB, HSPA5, PDIA4, CANX
hsa04610	Complement and coagulation cascades	12	[b]1.50×10^{-3}	KNG1, C8B, C7, A2M, FGA, C3, CFB, CD46, C6, SERPING1, C1S, C2
hsa04520	Adherens junction	12	[b]1.91×10^{-3}	ACTB, ACTG1, PTPN6, TGFBR2, CTNND1, CDH1, SMAD2, PTPN1, WASL, TCF7L2, IQGAP1, VCL
hsa05142	Chagas disease (American trypanosomiasis)	15	[b]1.98×10^{-3}	CFLAR, GNAI3, GNAI2, C3, RELA, TGFBR2, MAP2K4, NFKB1, SMAD2, CALR, GNAQ, PPP2CB, IL12A, PPP2R2B, PPP2R2A
hsa05110	Vibrio cholerae infection	10	[b]2.23×10^{-3}	ACTB, ACTG1, ATP6V1A, KDELR2, ATP6AP1, PRKCG, PRKACB, PDIA4, ATP6V1B1, TJP2
hsa05146	Amoebiasis	15	[b]2.37×10^{-3}	IL1R1, RELA, PRKCG, NFKB1, ITGAM, VCL, ARG1, C8B, SERPINB9, GNAQ, IL12A, PRKACB, COL1A1, CD14, FN1

B, Downregulated DEGs

hsa05412	Arrhythmogenic right ventricular cardiomyopathy (ARVC)	8	[b]2.35×10^{-3}	ITGA8, SGCD, DSC2, GJA1, ITGA2, CACNB4, ITGA4, CACNA1C
hsa04070	Phosphatidylinositol signaling system	9	[b]5.51×10^{-3}	PIK3CG, MTM1, DGKB, PIK3C2G, IMPA1, PIP5K1B, ITPKB, PTEN, ITPR2
hsa00562	Inositol phosphate metabolism	7	[a]1.33×10^{-2}	PIK3CG, MTM1, PIK3C2G, IMPA1, PIP5K1B, ITPKB, PTEN
hsa04020	Calcium signaling pathway	11	[a]2.61×10^{-2}	P2RX7, SLC8A1, CCKBR, ERBB4, PHKB, GRPR, ITPKB, PPP3CA, PTGFR, CACNA1C, ITPR2
hsa05202	Transcriptional misregulation in cancer	10	[a]4.13×10^{-2}	MAF, CCNT2, CSF2, HHEX, LMO2, FLT3, GZMB, SMAD1, JMJD1C, HMGA2

Table III. Continued.

Pathway	Name	Gene count	P-value	Genes
hsa04151	PI3K-Akt signaling pathway	16	[a]$5.39x10^{-2}$	PHLPP1, PIK3CG, COL4A3, PPP2R5A, TCL1A, ITGA2, FGF13, ITGA4, KIT, PTEN, COL5A2, PRLR, ITGA8, PDGFD, GHR, IL2
hsa05410	Hypertrophic cardiomyopathy (HCM)	6	[a]$6.39x10^{-2}$	ITGA8, SGCD, ITGA2, CACNB4, ITGA4, CACNA1C
hsa04810	Regulation of actin cytoskeleton	11	[a]$6.54x10^{-2}$	PIK3CG, DOCK1, ARHGEF7, DIAPH2, ITGA8, PIP5K1B, ITGA2, IQGAP2, FGF13, PDGFD, ITGA4
hsa04080	Neuroactive ligand-receptor interaction	13	[a]$8.12x10^{-2}$	CCKBR, NPY2R, GABRA5, PTGFR, P2RX7, AGTR2, P2RY10, PRLR, GRPR, CHRNA5, CHRNB3, TSHR, GHR
hsa05414	Dilated cardiomyopathy	6	[a]$8.21x10^{-2}$	ITGA8, SGCD, ITGA2, CACNB4, ITGA4, CACNA1C

[a]P<0.05, [b]P<0.01, [c]P<0.001. DEGs, differentially expressed genes.

the secondary site, tumor cells adhere to the secondary site, proliferate and eventually metastasize (16,17). Cell adhesion, receptor complex, integral component of plasma membrane, postsynaptic density and epidermal growth factor receptor binding are key auxiliary components (18-20). Cell adhesion molecules suppress the adhesive function of tumor cells and glycoproteins located on the cell surface (21). Moreover, KEGG pathway analysis indicated that the upregulated DEGs influenced 'protein processing in endoplasmic reticulum', 'antigen processing and presentation' and 'phagosome'; the downregulated DEGs were associated with 'arrhythmogenic right ventricular cardiomyopathy', 'phosphatidylinositol signaling system' and 'inositol phosphate metabolism'. Tumor metastasis involves detachment from the primary site of the tumor, entrance into the surrounding stroma and the circulation or lymphatic system, adhesion to endothelial cell walls, extravasation and invasion through vascular proliferation for the formation a novel metastatic lesion (22,23). GO and KEGG analyses suggested that the aforementioned DEGs may influence signaling pathways associated with tumor cell metastasis. The identified DEGs may provide novel research directions and targets for the treatment of HCC metastasis.

Based on the established PPI network with DEGs, the following top 10 hub genes were identified: HSPA8, PHLPP1, GART, CAD, ACTB, CDH1, PIK3CG, NFκB1, STAT3 and HSPA5. HSPA8 is a member of the heat shock proteins family, which influences molecular signal transduction, apoptosis and protein regulation (24). HSPA8 is located in the cytoplasm and lysosomes and is involved in mediating cell autophagy by binding to the substrate protein and transporting it into the lysosomal cavity (25,26). Novel research has shown that the Hsp70 protein may inhibit apoptosis by regulating the caspase-dependent pathway (27). Moreover, tumor vaccines against HSP70S have been successfully completed in animal models and clinical trials are underway (27).

PHLPP1 is an important regulator of Akt serine-threonine kinases and conventional/novel protein kinase C isoforms (28). PHLPP1 can inhibit growth factor-induced signal transduction pathways in cancer cells, so it may be used as a growth inhibitor in several types of cancer (28). In the human breast cancer cell line 21T, AK294 phosphorylation was inhibited by LY294002, and the expression of PHLPP1 in two metastatic cell lines (MT1 and MT2) was much lower compared with early breast cancer cells (29). PHLPP1 can negatively regulate the activity of AKT and its downstream kinase by phosphorylating the hydrophobic group of AKT at the Serine473 site. This resulted in inhibition of the PI3K/AKT signaling pathway, and the activation of various cancer promoting signaling pathways, including amplification or gain-of-function mutations in upstream receptor protein tyrosine kinases (RPTKs), activating mutations in PI3K and Akt and loss-of-function mutations in the regulatory phosphatase PTEN, which affect differentiation and proliferation of cancer cells and apoptosis in breast cancer cells (29). Therefore, it is hypothesized that PHLPP1 is associated with tumor metastasis.

Trifunctional purine biosynthetic protein adenosine-3 is an enzyme that is encoded by the GART gene (30). GART participates in several aspects of energy metabolism, including as a ATP binding source, metal ion

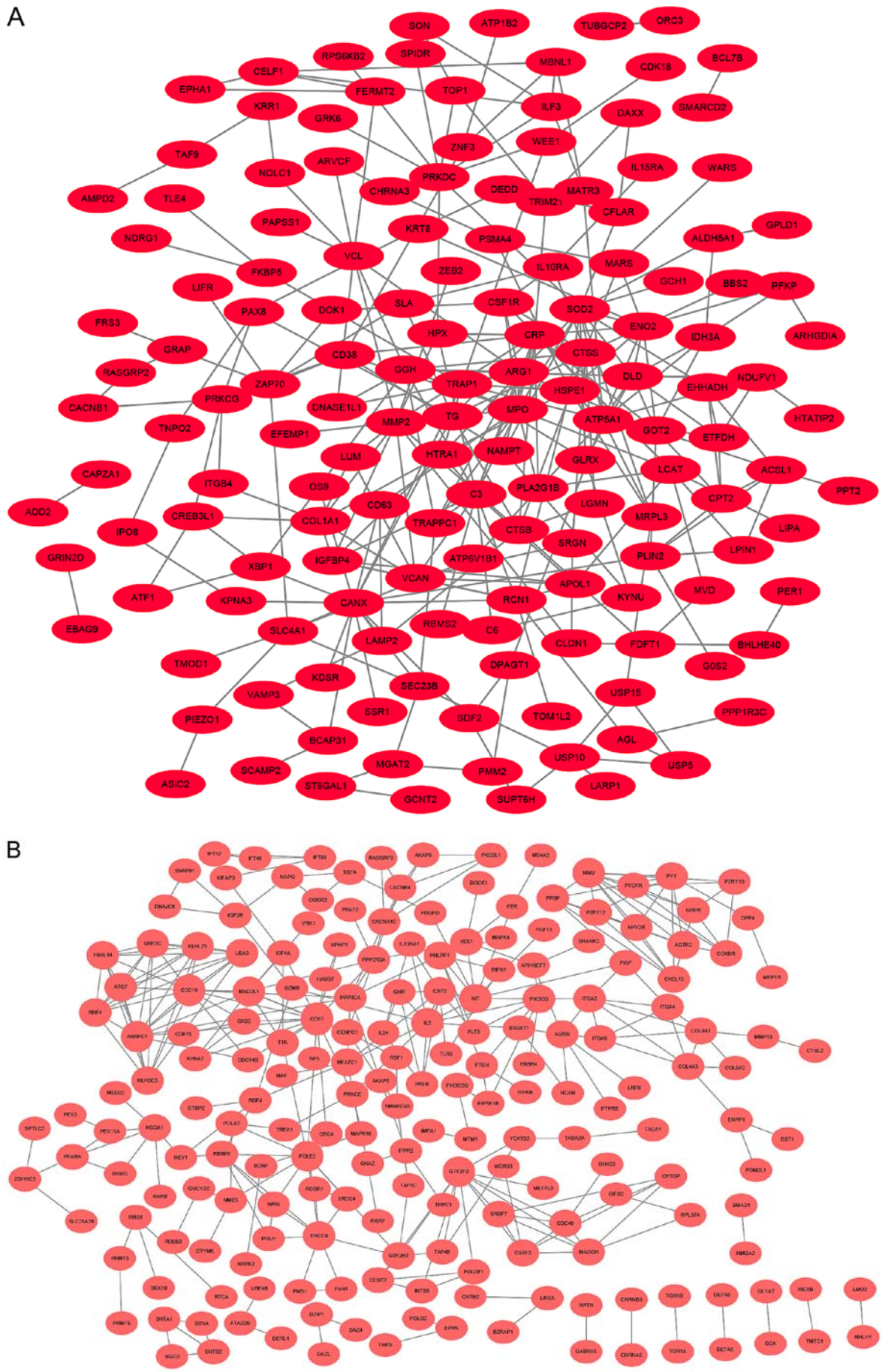

Figure 2. DEG protein-protein interaction network in metastasis-inclined microenvironment and metastasis-averse microenvironment. (A) The most significant interaction network of the upregulated DEGs interaction network. (B) Interaction network of the 317 downregulated DEGs interaction network. DEG, differentially expressed gene.

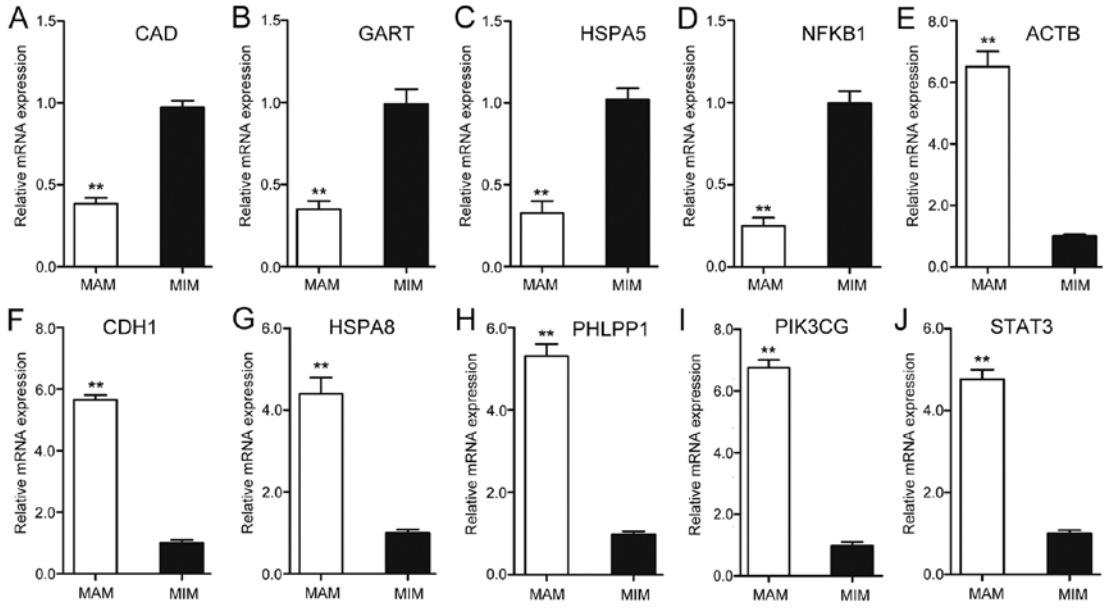

Figure 3. Top 10 hub genes were detected by reverse transcription-quantitative PCR. Expression of (A) CAD, (B) GART, (C) HSPA5, (D) NFKB1, (E) ACTB, (F) CDH1, (G) HSPA8, (H) PHLPP1, (I) PIK3GC and (J) STAT3 The data are presented as the mean ± standard deviation of 3 independent experiments. **P<0.01 MAM vs. MIM. CAD, carbamoyl-phosphate synthetase 2; GART, phosphoribosylglycinamide formyltransferase; HSPA5, heat shock protein family A member 5; NFκB1, nuclear factor κB subunit 1; ACTB, actin beta; CDH1, Cadherin 1; HSPA8, heat shock protein family A member 8; PHLPP1, PH domain and leucine rich repeat protein phosphatase 1; PIK3CG, phosphatidylinositol-4,5-bisphosphate 3-kinase catalytic subunit γ; STAT3, signal transducer and activator of transcription 3.

binding source and phosphoribosylamine-glycine ligase activity source (30,31). CAD is a fusion gene that encodes three enzymes involved in pyrimidine biosynthesis; carbamoyl-phosphate synthetase 2 and aspartate transcarbamylase fused with dihydroorotase (31). CAD is a key enzyme the regulates multiple biological processes in the first three steps of pyrimidine biosynthesis (32). These three genes serve a role in the synthesis and metabolism of nucleic acids and proteins in cells, and their synthesized products provide essential substances and energy for cell proliferation (32).

Actin is a major constituent of the muscular contractile apparatus and ACTB is one of six different actin isoforms that have been identified in humans (33). ACTB binds RNA-binding protein Sam68 and participates in the regulation of the synaptic formation of dendritic spines (34). ACTB supports the muscular cytoskeleton during the formation of novel tumor cells following tumor cell proliferation and metastasis. Thus, ACTB is considered to be associated with cell proliferation and metastasis (34).

CDH1, also known as epithelial cadherin (E-cadherin), is a protein encoded by the CDH1 gene (35). Mutations in CDH1 are closely associated with liver, colorectal and gastric cancer. Moreover, a functional deficit of CDH1 promotes the proliferation and invasiveness of tumor cells, and promotes the malignant development of tumors (35). E-cadherin is a member of the cadherin family and downregulation of E-cadherin reduces cell-cell adhesion, which results in cells that are more susceptible to migration (36). This change can easily result in cancer cells passing through the cell basement membrane and invading surrounding tissues (36). A previous study demonstrated that E-cadherin is an important protein that regulates cell-cell adhesion. On the cell membrane, E-cadherin binds to β-catenin via its cytoplasmic tail, allowing epithelial cells to bind tightly together. Knockdown of E-cadherin expression results in β-catenin release into the cytoplasm and translocation into the nucleus, and this process can result in the expression of epithelial mesenchymal transition (EMT)-inducible transcription factors. Therefore, E-cadherin is an important gene that regulates EMT (37).

The PIK3CG subunit λ isoform is an enzyme encoded by the PIK3CG gene (38). Several studies have demonstrated that the function of PIK3CG is to regulate the transmission of extracellular signals, including E-cadherin-mediated cell-cell adhesion, which serves an important role in maintaining the structural and functional integrity of the epithelium (39,40).

The NFκB1 gene is a cellular transcription factor and encodes the NF-κB p105 subunit protein. The expression of NF-κB is activated via various stimuli, such as cytokines, oxidative free radicals and bacterial or viral products (41). Activated NF-κB is transported to the nucleus to participate in the transcription and synthesis of various proteins and signaling molecules, regulating various cell behaviors (41). It has been revealed that osteopontin can regulate the expression of MTI-MMP via the NF-κB signaling pathway and promote the migration of cancer cells and invasion into the extracellular matrix (42). A previous study confirmed that several adhesion molecules, such as ICAM-1, VCAM-1 and ELAM-1, are regulated by NF-κB, which serves an important role in tumor metastasis (43).

STAT3, which contains SH2 and SH3 domains, binds to specific phosphotyrosine-containing peptides. When STAT3 is activated by phosphorylation, it serves as a transcriptional activator, in either its homodimeric or heterodimeric form (44). Phosphorylated STAT3 binds a specific site in the target gene promoter sequence and promotes transcription of the gene (44). Dysregulation of this pathway in tumors leads

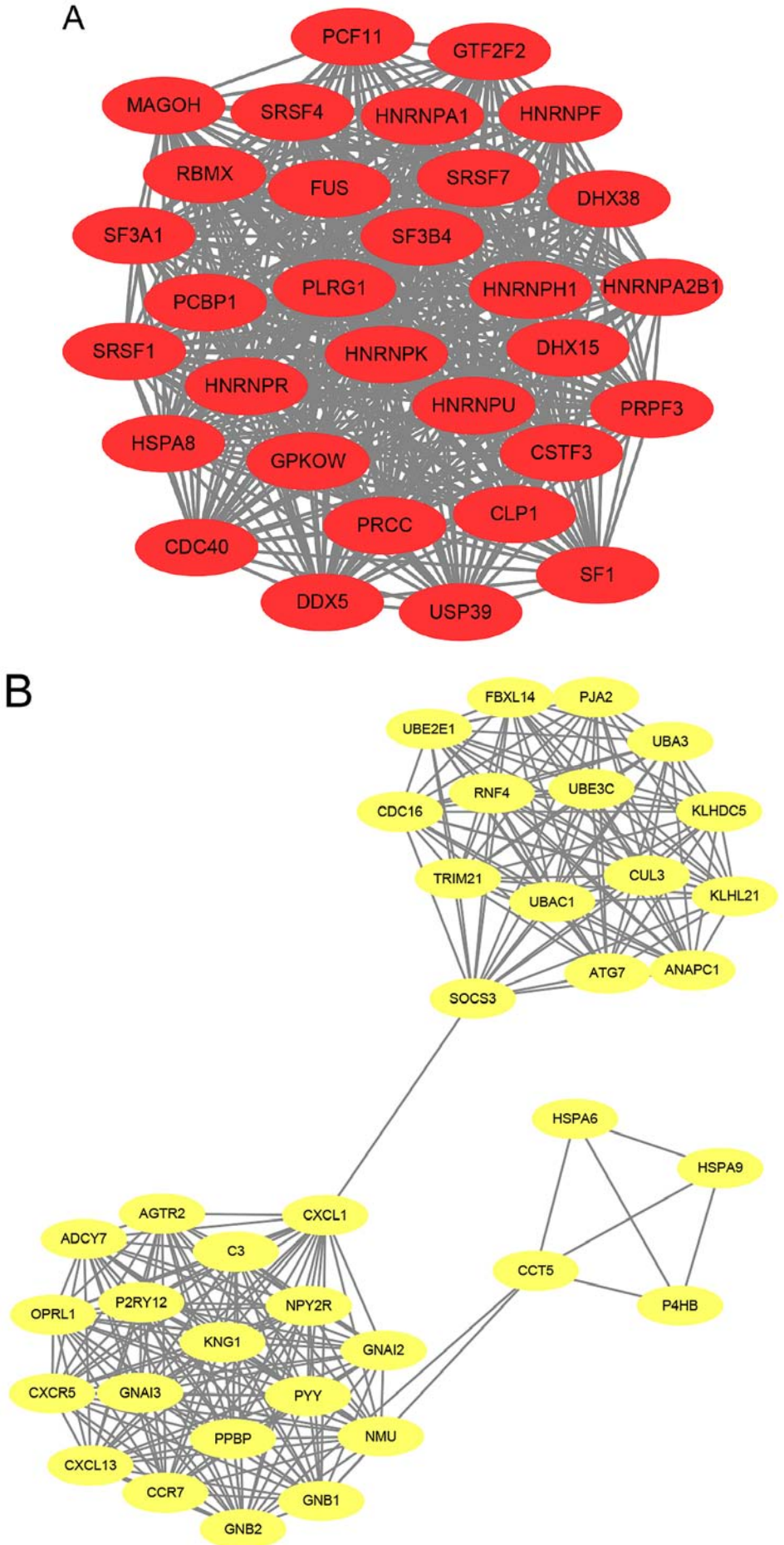

Figure 4. Top 3 modules from the protein-protein interaction network determined by the molecular complex detection score. (A) Module 1 and (B) Module 2.

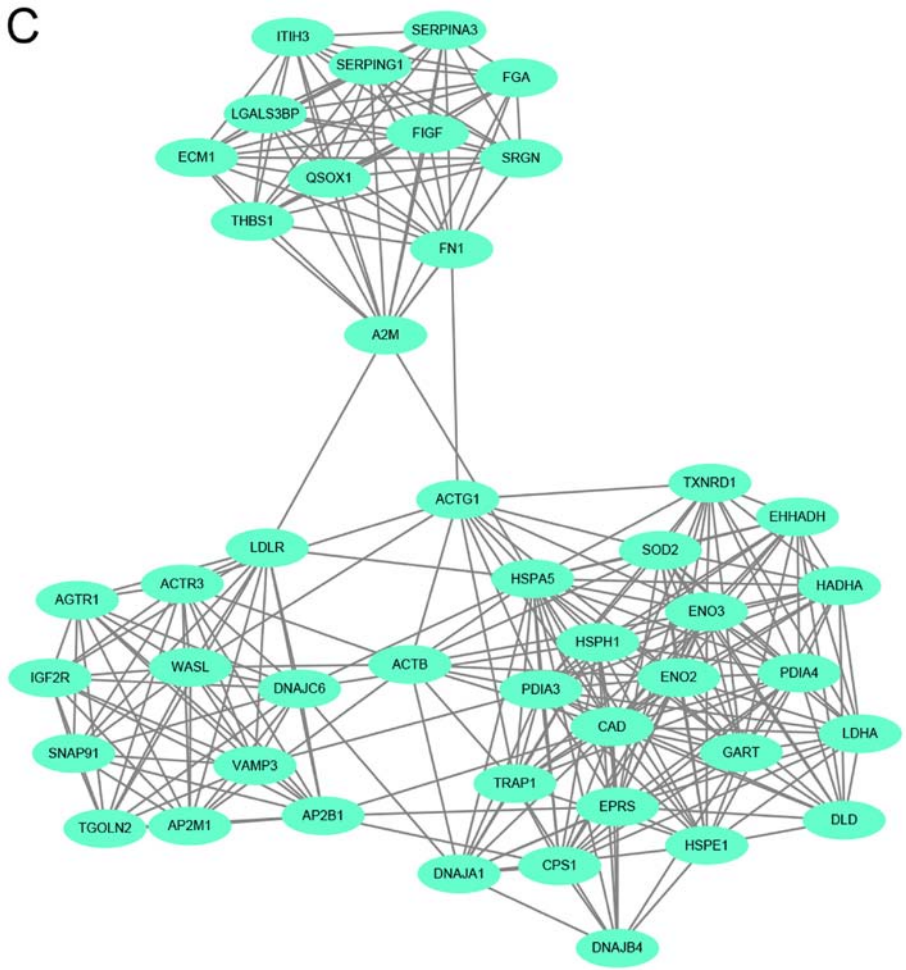

Figure 4. Continued. Top 3 modules from the protein-protein interaction network determined by the molecular complex detection score. (C) Module 3.

Table IV. Functional and pathway enrichment analysis of the genes in module 1.

Category	Term	Gene function	Gene count	P-value
BP	GO:0008380	RNA splicing	6	$^{c}2.27\times10^{-9}$
BP	GO: 0000398	mRNA splicing, via spliceosome	6	$^{c}8.01\times10^{-7}$
BP	GO:0006397	mRNA processing	5	$^{c}2.06\times10^{-6}$
BP	GO:0048025	Negative regulation of mRNA splicing, via spliceosome	4	$^{c}3.81\times10^{-6}$
BP	GO:0000381	Regulation of alternative mRNA splicing, via spliceosome	4	$^{c}4.06\times10^{-5}$
CC	GO:0071013	Catalytic step 2 spliceosome	3	$^{c}6.60\times10^{-19}$
CC	GO:0005681	Spliceosomal complex	2	$^{c}1.58\times10^{-10}$
CC	GO:0030529	Intracellular ribonucleoprotein complex	2	$^{c}8.66\times10^{-9}$
CC	GO:0019013	Viral nucleocapsid	2	$^{c}7.85\times10^{-8}$
CC	GO:0005654	Nucleoplasm	12	$^{c}8.50\times10^{-6}$
MF	GO:0000166	Nucleotide binding	7	$^{c}3.01\times10^{-10}$
MF	GO:0044822	Poly(A) RNA binding	7	$^{c}1.66\times10^{-9}$
MF	GO:0003723	RNA binding	6	$^{c}1.95\times10^{-5}$
MF	GO:0003729	mRNA binding	12	$^{c}4.65\times10^{-5}$
MF	GO:0003676	Nucleic acid binding	7	$^{c}8.67\times10^{-4}$
KEGG_PATHWAY	has:03040	Spliceosome	20	$^{c}1.54\times10^{-28}$
KEGG_PATHWAY	has: 03015	mRNA surveillance pathway	4	$^{b}4.32\times10^{-3}$
KEGG_PATHWAY	has: 05168	Herpes simplex infection	4	$^{a}3.18\times10^{-2}$

^{a}P<0.05, ^{b}P<0.01, ^{c}P<0.001. GO, Gene Ontology; BP, biological process; CC, cellular component; MF, molecular function; KEGG, Kyoto Encyclopedia of Genes and Genomes.

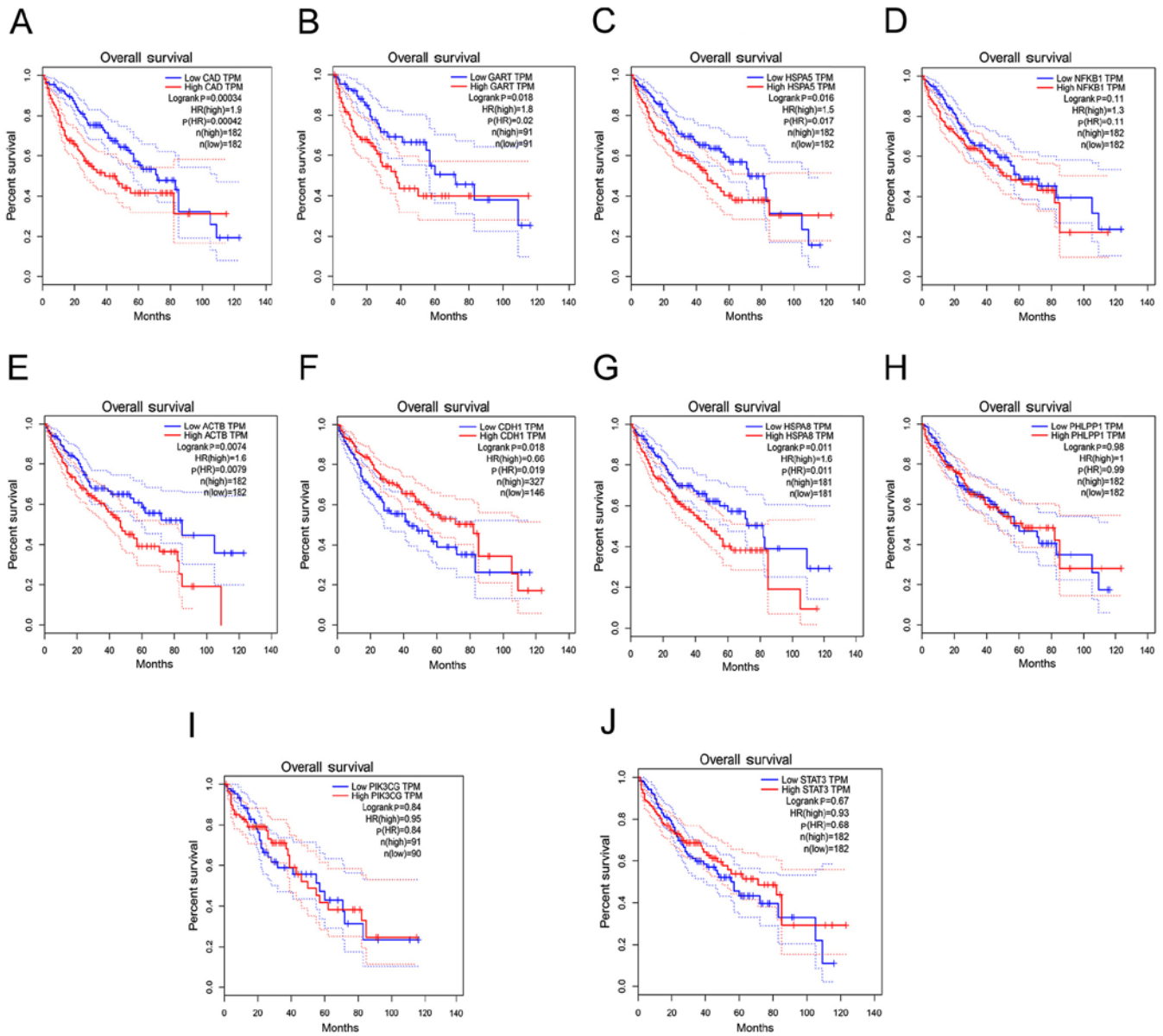

Figure 5. Prognostic value of hub genes in patients with HCC. Kaplan-Meier analysis of OS time un patients with HCC with high and low expression levels of: (A) CAD, (B) GART, (C) HSPA5, (D) NFκB1, (E) ACTB, (F) CDH1, (G) HSPA8, (H) PHLPP1, (I) PIK3CG and (J) STAT3. The red dotted line above the red curve and the red dotted line below represent the high (50%) and low cutoff (50%) on the survival curve. The blue dotted line above the blue curve and the blue dotted line below represent high (50%) and low cutoff (50%) on the survival curve. HCC, hepatocellular carcinoma; OS, overall survival; CAD, carbamoyl-phosphate synthetase 2; GART, phosphoribosylglycinamide formyltransferase; HSPA5, heat shock protein family A member 5; NFκB1, nuclear factor κB subunit 1; ACTB, actin beta; CDH1, cadherin 1; HSPA8, heat shock protein family A member 8; PHLPP1, PH domain and leucine rich repeat protein phosphatase 1; PIK3CG, phosphatidylinositol-4,5-bisphosphate 3-kinase catalytic subunit γ; STAT3, signal transducer and activator of transcription 3; HR, hazard ratio; TPM, transcripts per million.

to increased angiogenesis surrounding the tumor, promotes blood supply to the tumor, increases tumor survival and promotes malignant development. It has been demonstrated that tissue-specific inactivation of STAT3 in the lungs of mice is associated with the occurrence and progression of lung adenocarcinoma, which reduced the survival rate. Notably, decreased expression of STAT3 promotes the expression of NF-κB in the cytoplasm, thus regulating NF-κB-induced IL-8 expression (45). This process promotes IL-8-mediated tumor invasion, angiogenesis and progression (45).

Binding immunoglobulin protein, also known as HSPA5, is a protein that is encoded by the HSPA5 gene (46). A large number of studies have revealed the high expression of HSPA5 in all malignant tumors (47,48). Therefore, inhibiting HSPA5 gene expression may be used as an adjuvant therapy for cancer. In addition, reducing the large amount of HSPA5 produced during the stress response can increase the apoptosis of tumor cells and inhibit tumor growth (49).

In addition, tumor metastasis is a complex multi-step process, whereby tumor cells not only interact with each other and host cells, but also with extracellular matrix components (50). Certain characteristics, such as adhesion, metastasis, migration, skeleton assembly, signal transduction and proliferation are associated with tumor metastasis (50,51). Migration is considered a key factor in the process of tumor cell metastasis (51). Previous studies have demonstrated

Table V. Functional and pathway enrichment analysis of the genes in module 2.

Category	Term	Gene function	Gene count	P-value
BP	GO:0032446	Protein modification by small protein conjugation	12	[b]6.57×10^{-9}
BP	GO:0070647	Protein modification by small protein conjugation or removal	12	[b]5.38×10^{-8}
BP	GO:0007186	G-protein coupled receptor signaling pathway	11	[b]2.93×10^{-7}
BP	GO:0016567	Protein ubiquitination	10	[b]5.90×10^{-7}
BP	GO:0007193	Adenylate cyclase-inhibiting G-protein coupled receptor signaling pathway	5	[b]6.02×10^{-6}
CC	GO:1902494	Catalytic complex	11	[b]9.45×10^{-6}
CC	GO:0000151	Ubiquitin ligase complex	7	[b]1.07×10^{-5}
CC	GO:0098552	Side of membrane	5	[b]2.94×10^{-4}
CC	GO:1990234	Transferase complex	6	[b]3.96×10^{-4}
CC	GO:0000152	Nuclear ubiquitin ligase complex	3	[a]1.53×10^{-3}
MF	GO:0004842	Ubiquitin-protein transferase activity	8	[b]3.79×10^{-6}
MF	GO:0001664	G-protein coupled receptor binding	6	[b]4.47×10^{-6}
MF	GO:0019787	Ubiquitin-like protein transferase activity	8	[b]5.20×10^{-6}
MF	GO:0008528	G-protein coupled peptide receptor activity	5	[b]1.42×10^{-4}
MF	GO:0001653	Peptide receptor activity	5	[b]1.52×10^{-4}
KEGG_PATHWAY	has: 04062	Chemokine signaling pathway	11	[b]4.43×10^{-10}
KEGG_PATHWAY	has: 04120	Ubiquitin mediated proteolysis	6	[b]1.26×10^{-4}
KEGG_PATHWAY	has: 04914	Progesterone-mediated oocyte maturation	5	[b]2.19×10^{-4}

[a]P<0.01, [b]P<0.001. GO, gene ontology; BP, biological process; CC, cellular component; MF, molecular function; KEGG, Kyoto Encyclopedia of Genes and Genomes.

Table VI. Functional and pathway enrichment analysis of the genes in module 3.

Category	Term	Gene function	Gene count	P-value
BP	GO:0006457	Protein folding	8	[b]1.45×10^{-7}
BP	GO:0045454	Cell redox homeostasis	5	[b]3.19×10^{-5}
BP	GO:0044710	Single-organism metabolic process	19	[b]4.36×10^{-5}
BP	GO:0006091	Generation of precursor metabolites and energy	6	[b]3.46×10^{-4}
BP	GO:0090066	Regulation of anatomical structure size	7	[b]3.49×10^{-4}
CC	GO:0070062	Extracellular exosome	23	[b]1.72×10^{-8}
CC	GO:0072562	Blood microparticle	5	[b]7.56×10^{-5}
CC	GO:0005577	Fibrinogen complex	3	[b]1.64×10^{-4}
CC	GO:0043209	Myelin sheath	5	[b]5.65×10^{-4}
CC	GO:0005829	Cytosol	9	[a]2.90×10^{-3}
MF	GO:0003756	Protein disulfide isomerase activity	3	[a]1.07×10^{-3}
MF	GO:0005524	ATP binding	11	[a]1.31×10^{-3}
MF	GO:0004070	Aspartate carbamoyltransferase activity	2	[a]5.77×10^{-3}
MF	GO:0004088	Carbamoyl-phosphatesynthase (glutamine-hydrolyzing) activity	2	[a]5.77×10^{-3}
MF	GO:0004087	Carbon metabolism	2	[a]5.77×10^{-3}
KEGG_PATHWAY	has: 01200	Chemokine signaling pathway	5	[a]1.23×10^{-3}
KEGG_PATHWAY	has: 04144	Endocytosis	6	[a]2.89×10^{-3}
KEGG_PATHWAY	has: 05100	Bacterial invasion of epithelial cells	4	[a]4.33×10^{-3}

[a]P<0.01, [b]P<0.001. GO, gene ontology; BP, biological process; CC, cellular component; MF, molecular function; KEGG, Kyoto Encyclopedia of Genes and Genomes.

that RNA splicing, protein modification by small protein conjugation, catalytic complex, ubiquitin-protein transferase activity, chemokine signaling pathways, protein folding, extracellular exosomes, protein disulfide isomerase activity and chemokine signaling pathways are also involved in the process of tumor cell migration and metastasis, such as the expansion of the cell front, the formation of new adhesion sites and the release of the original adhesion sites in the tail of the cell (52-56).

A study reported that miR-26b-5p exerts metastatic properties and maintains epithelial cell adhesion molecule + cancer stem cells via HSPA8 in HCC (57). Moreover, a study investigating the role of PHLPP1 in HCC reported that miR-190 influences EMT by regulating the expression of PHLPP1, thus affecting the malignant biological behavior of HCC cells (58). Isobaric tags for relative and absolute quantification analysis of clinical samples of HCC indicated that ACTB serves an important role in the initiation stage of HCC (59). Long non-coding RNA ATRERNA1 promotes the metastasis and invasiveness of HCC cells by recruiting EHMT2 and/or ehmt2/snai1 complexes to inhibit CDH1 (60). Loss of NFκB1 promotes the occurrence of age-related chronic liver disease (CLD) which is characterized by steatosis, neutrophil proliferation, fibrosis, telomere damage of hepatocytes and HCC (61). The results of the present study demonstrated that STAT3 is one of the hub genes. Phosphorylated RPN2 activates the signal transducer and activator of STAT3 and is also responsible for the RPN2-stimulated elevated expression of MMP-9 and for invading HCC cells (62).

In the current study, biological function and signal pathway enrichment analysis revealed that the genes in module 1, 2 and 3 were primarily enriched in 'RNA splicing', 'G-protein coupled receptor signaling pathway' and 'protein ubiquitination'. Studies have demonstrated that these signaling pathways are required for cell survival and metabolism and serve an important role in tumor recurrence and metastasis (63-65). Therefore, it is hypothesized that these molecular pathways may provide novel insight and potential targets for the diagnosis and treatment of HCC.

In conclusion, 1,171 DEGs were identified (including 712 upregulated and 459 downregulated genes, 1,033 nodes, 7,589 edges and 10 hub genes) via gene profile dataset and integrated bioinformatics analysis in noncancerous surrounding hepatic tissues. The 10 hub genes were significantly enriched in several signaling pathways which serve an important role in tumor metastasis. According to the present research and analysis, CAD, GART, HSPA5, ACTB, CDH1 and HSPA8 may have potential as targets for the diagnosis and treatment of metastatic HCC. The present study may provide a scientific basis for the investigation of these genes in HCC in the future.

Acknowledgements

Not applicable.

Funding

The present study was supported by The Foundation of Scientific Research of Sichuan Medical Association (grant. no. S16007), The Sichuan Health Planning Commission Key Project Foundation (grant. no. 17ZD008), The Sichuan Science and Technology Project (grant. no. 2018JY0276) and The Chengdu Science and Technology Bureau Technology Innovation Project (grant. no. 2018-YF05-01228-SN).

Availability of data and materials

The datasets generated and/or analyzed during the present study are available in the [NCBI] repository, [https://www.ncbi.nlm.nih.gov/geo].

Authors' contributions

YL and HW performed the experiments, analyzed the data and drafted the manuscript. YW, HW, MD and CL conceptualized the study design and critically revised the manuscript. YL, MD, CL and HW wrote the manuscript. All authors read and approved the final manuscript.

Ethics approval and consent to participate

The present study was approved by The Institutional Review Board of the Second Affiliated Hospital of Chongqing Medical University (Chongqing, China) and written informed consent was provided by all patients according to the Declaration of Helsinki.

Patient consent for publication

Not applicable.

Competing interests

The authors declare that they have no competing interests.

References

1. Siegel RL, Miller KD and Jemal A: Cancer statistics, 2016. CA Cancer J Clin 66: 7-30, 2016.
2. Chen WQ, Zheng RS, Baade PD, Zhang S, Zeng H, Bray F, Jemal A, Yu XQ and He J: Cancer statistics in China, 2015. CA Cancer J Clin 66: 115-132, 2016.
3. Greten TF, Wang XW and Korangy F: Current concepts of immune based treatments for patients with HCC: From basic science to novel treatment approaches. Gut 64: 842-848, 2015.
4. Pang RW, Joh JW, Johnson PJ, Monden M, Pawlik TM and Poon RT: Biology of hepatocellular carcinoma. Ann Surg Oncol 15: 962-971, 2008.
5. Ye QH, Qin LX, Forgues M, He P, Kim JW, Peng AC, Simon R, Li Y, Robles AI, Chen Y, *et al*: Predicting hepatitis B virus-positive metastatic hepatocellular carcinomas using gene expression profiling and supervised machine learning. Nat Med 9: 416-423, 2003.
6. Iizuka N, Oka M, Yamada-Okabe H, Nishida M, Maeda Y, Mori N, Takao T, Tamesa T, Tangoku A, Tabuchi H, *et al*: Oligonucleotide microarray for prediction of early intrahepatic recurrence of hepatocellular carcinoma after curative resection. Lancet 361: 923-929, 2003.
7. Budhu A, Forgues M, Ye QH, Jia HL, He P, Zanetti KA, Kammula US, Chen Y, Qin LX, Tang ZY and Wang XW: Prediction of venous metastases, recurrence, and prognosis in hepatocellular carcinoma based on a unique immune response signature of the liver microenvironment. Cancer Cell 10: 99-111, 2006.
8. Tang Z, Li C, Kang B, Gao G, Li C and Zhang Z: GEPIA: A web server for cancer and normal gene expression profiling and interactive analyses. Nucleic Acids Res 45(W1): W98-W102, 2017.

9. Szklarczyk D, Gable AL, Lyon D, Junge A, Wyder S, Huerta-Cepas J, Simonovic M, Doncheva NT, Morris JH, Bork P, *et al*: STRING v11: Protein-protein association networks with increased coverage, supporting functional discovery in genome-wide experimental datasets. Nucleic Acids Res 47: D607-D613, 2019.
10. Shannon P, Markiel A, Ozier O, Baliga NS, Wang JT, Ramage D, Amin N, Schwikowski B and Ideker T: Cytoscape: A software environment for integrated models of biomolecular interaction networks. Genome Res 13: 2498-2504, 2003.
11. Bader GD and Hogue CW: An automated method for finding molecular complexes in large protein interaction networks. BMC Bioinformatics 4: 2, 2003.
12. Livak KJ and Schmittgen TD: Analysis of relative gene expression data using real-time quantitative PCR and the 2(-Delta Delta C(T)) method. Methods 25: 402-408, 2001.
13. Thorgeirsson SS and Grisham JW: Molecular pathogenesis of human hepatocellular carcinoma. Nat Genet 31: 339-346, 2002.
14. Fan W and Ye G: Microarray analysis for the identification of specific proteins and functional modules involved in the process of hepatocellular carcinoma originating from cirrhotic liver. Mol Med Rep 17: 5619-5626, 2018.
15. Gulubova MV: Expression of cell adhesion molecules, their ligands and tumour necrosis factor alpha in the liver of patients with metastatic gastrointestinal carcinomas. Histochem J 34: 67-77, 2002.
16. Ploverini P: Cellular adhesion molecules; newly identified mediators of angiogenesis. Am J Pathol 148: 1023-1029, 1996.
17. McGrogan D and Bookstein R: Tumor suppressor genes in prostate cancer. Semin Cancer Biol 8: 11-19, 1997.
18. Folkman J: Tumor angiogenesis: Therapeutic implications. N Engl J Med 285: 1182-1186, 1971.
19. Folkman J: What is the evidence that tumors are angiogenesis dependent? J Natl Cancer Inst 82: 4-6, 1990.
20. Akiyama SK, Larjava H and Yamada KM: Differences in the biosynthesis and localization of the fibronectin receptor in normal and transformed cultured human cells. Cancer Res 50: 1601-1607, 1990.
21. Koop S, Schmidt EE, MacDonald IC, Morris VL, Khokha R, Grattan M, Leone J, Chambers AF and Groom AC: Independence of metastatic ability and extravasation: Metastatic ras-transformed and control fibroblasts extravasate equally well. Proc Natl Acad Sci USA 93: 11080-11084, 1996.
22. Klein CA: Cancer. The metastasis cascade. Science 321: 1785-1787, 2008.
23. Chiang AC and Massagué J: Molecular basis of metastasis. N Engl J Med 359: 2814-2823, 2008.
24. O'Donnell JP, Marsh HM, Sondermann H and Sevier CS: Disrupted hydrogen-bond network and impaired ATPase activity in an Hsc70 cysteine mutant. Biochemistry 57: 1073-1086, 2018.
25. Mayer MP and Bukau B: Hsp70 chaperones: Cellular functions and molecular mechanism. Cell Mol Life Sci 62: 670-684, 2005.
26. Xie W, Zhang L, Jiao H, Guan L, Zha J, Li X, Wu M, Wang Z, Han J and You H: Chaperone-mediated autophagy prevents apoptosis by degrading BBC3/PUMA. Autophagy 11: 1623-1635, 2015.
27. Majeski AE and Dice JF: Mechanisms of chaperone-mediated autophagy. Int J Biochem Cell Biol 36: 2435-2444, 2004.
28. Wang X, Wang Q, Lin H, Li S, Sun L and Yang Y: HSP72 and gp96 in gastroenterological cancers. Clin Chim Acta 417: 73-79, 2013.
29. Brognard J and Newton AC: PHLiPPing the switch on Akt and protein kinase C signaling. Trends Endocrinol Metab 19: 223-230, 2008.
30. Qiao M, Iglehart JD and Pardee AB: Metastatic potential of 21T human breast cancer cells depends on Akt/protein kinase B activation. Cancer Res 67: 5293-5299, 2007.
31. Hattori M, Fujiyama A, Taylor TD, Watanabe H, Yada T, Park HS, Toyoda A, Ishii K, Totoki Y, Choi DK, *et al*: The DNA sequence of human chromosome 21. Nature 405: 311-319, 2000.
32. Banerjee D and Nandagopal K: Potential interaction between the GARS-AIRS-GART Gene and CP2/LBP-1c/LSF transcription factor in down syndrome-related Alzheimer disease. Cell Mol Neurobiol 27: 1117-1126, 2007.
33. Ng BG, Wolfe LA, Ichikawa M, Markello T, He M, Tifft CJ, Gahl WA and Freeze HH: Biallelic mutations in CAD, impair de novo pyrimidine biosynthesis and decrease glycosylation precursors. Hum Mol Genet 24: 3050-3057, 2015.
34. Gunning PW, Ghoshdastider U, Whitaker S, Popp D and Robinson RC: The evolution of compositionally and functionally distinct actin filaments. J Cell Sci 128: 2009-2019, 2015
35. Guo C, Liu S, Wang J, Sun MZ and Greenaway FT: ACTB in cancer. Clin Chim Acta 417: 39-44, 2013.
36. Cappell SD, Chung M, Jaimovich A, Spencer SL and Meyer T: Irreversible APC (Cdh1) inactivation underlies the point of no return for cell-cycle entry. Cell 166: 167-180, 2016.
37. Beavon IR: The E-cadherin-catenin complex in tumour metastasis: Structure, function and regulation. Eur J Cancer 36: 1607-1620, 2000.
38. Polyak K and Weinberg RA: Transitions between epithelial and mesenchymal states: Acquisition of malignant and stem cell traits. Nat Rev Cancer 9: 265-273, 2009.
39. Alloatti G, Montrucchio G, Lembo G and Hirsch E: Phosphoinositide 3-kinase gamma: Kinase-dependent and -independent activities in cardiovascular function and disease. Biochem Soc Trans 32: 383-386, 2004.
40. Rubio I, Wittig U, Meyer C, Heinze R, Kadereit D, Waldmann H, Downward J and Wetzker R: Farnesylation of Ras is important for the interaction with phosphoinositide 3-kinase gamma. Eur J Biochem 266: 70-82, 1999.
41. Uehara M, McGrath MM, Ohori S, Solhjou Z, Banouni N, Routray S, Evans C, DiNitto JP, Elkhal A, Turka LA, *et al*: Regulation of T cell alloimmunity by PI3Kγ and PI3Kδ. Nat Commun 8: 951, 2017.
42. Concetti J and Wilson CL: NFKB1 and cancer: Friend or foe? Cells 7: E133, 2018.
43. Philip S, Bulbule A and Kundu GC: Matrix metalloproteinase-2: Mechanism and regulation of NF-κB-mediated activation and its role in cell motility and ECM-invasion. Glycoconj J 21: 429-441, 2004.
44. Bharti AC and Aggarwal BB: Nuclear factor-kappa B and cancer: Its role in prevention and therapy. Biochem Pharmacol 64: 883-888, 2002.
45. Wang Y, Shen Y, Wang S, Shen Q and Zhou X: The role of STAT3 in leading the crosstalk between human cancers and the immune system. Cancer Lett 415: 117-128, 2018.
46. Caetano MS, Hassane M, Van HT, Bugarin E, Cumpian AM, McDowell CL, Cavazos CG, Zhang H, Deng S, Diao L, *et al*: Sex specific function of epithelial STAT3 signaling in pathogenesis of K-ras mutant lung cancer. Nat Commun 9: 4589, 2018.
47. Wang J, Lee J, Liem D and Ping P: HSPA5 gene encoding Hsp70 chaperone BiP in the endoplasmic reticulum. Gene 618: 14-23, 2017.
48. Arap MA, Lahdenranta J, Mintz PJ, Hajitou A, Sarkis AS, Arap W and Pasqualini R: Cell surface expression of the stress response chaperone GRP78 enables tumor targeting by circulating ligands. Cancer Cell 6: 275-284, 2004.
49. Shuda M, Kondoh N, Imazeki N, Tanaka K, Okada T, Mori K, Hada A, Arai M, Wakatsuki T, Matsubara O, *et al*: Activation of the ATF6, XBP1 and grp78 genes in human hepatocellular carcinoma: A possible involvement of the ER stress pathway in hepatocarcinogenesis. J Hepatol 38: 605-614, 2003.
50. Um E, Oh JM, Granick S and Cho YK: Cell migration in micro-engineered tumor environments. Lab Chip 17: 4171-4185, 2017.
51. Condeelis J and Pollard JW: Macrophages: Obligate partners for tumor cell migration, invasion, and metastasis. Cell 124: 263-266, 2006.
52. Yang Y, Zheng H, Zhan Y and Fan S: An emerging tumor invasion mechanism about the collective cell migration. Am J Transl Res 11: 5301-5312, 2019.
53. Denisenko TV, Gorbunova AS and Zhivotovsky B: Mitochondrial involvement in migration, invasion and metastasis. Front Cell Dev Biol 7: 355, 2019.
54. Li X, Miao Y, Pal DS and Devreotes PN: Excitable networks controlling cell migration during development and disease. Semin Cell Dev Biol: Dec 10, 2019 (Epub ahead of print). doi: 10.1016/j.semcdb.2019.11.001.
55. Mishra AK, Campanale JP, Mondo JA and Montell DJ: Cell interactions in collective cell migration. Development 146: dev172056, 2019.
56. Greenlee JD and King MR: Engineered fluidic systems to understand lymphatic cancer metastasis. Biomicrofluidics 14: 011502, 2020.
57. Misra UK, Payne S and Pizzo SV: The monomeric receptor binding domain of tetrameric; α2-macroglobulin binds to cell surface GRP78 triggering equivalent; activation of signaling cascades. Biochemistry 52: 4014-4025, 2013.
58. Khosla R, Hemati H, Rastogi A, Ramakrishna G, Sarin SK and Trehanpati N: MiR-26b-5p helps in EpCAM+cancer stem cells maintenance via HSC71/HSPA8 and augments malignant features in HCC. Liver Int 39: 1692-1703, 2019.

59. Xiong Y, Wu S, Yu H, Wu J, Wang Y, Li H, Huang H and Zhang H: MiR-190 promotes HCC proliferation and metastasis by targeting PHLPP1. Exp Cell Res 371: 185-195, 2018.
60. Goh WW, Lee YH, Ramdzan ZM, Chung MC, Wong L and Sergot MJ: A network-based maximum link approach towards MS identifies potentially important roles for undetected ARRB1/2 and ACTB in liver cancer progression. Int J Bioinform Res Appl 8: 155-170, 2012.
61. Song W, Gu Y, Lu S, Wu H, Cheng Z, Hu J, Qian Y, Zheng Y and Fan H: LncRNA TRERNA1 facilitates hepatocellular carcinoma metastasis by dimethylating H3K9 in the CDH1 promoter region via the recruitment of the EHMT2/SNAI1 complex. Cell Prolif 52: e12621, 2019.
62. Wilson CL, Jurk D, Fullard N, Banks P, Page A, Luli S, Elsharkawy AM, Gieling RG, Chakraborty JB, Fox C, *et al*: NFκB1 is a suppressor of neutrophil-driven hepatocellular carcinoma. Nat Commun 6: 6818, 2015.
63. Black DL: Mechanisms of alternative pre-messenger RNA splicing. Annu Rev Biochem 72: 291-336, 2003.
64. King N, Hittinger CT and Carroll SB: Evolution of key cell signaling and adhesion protein families predates animal origins. Science 301: 361-363, 2003.
65. Mukhopadhyay D and Riezman H: Proteasome-independent functions of ubiquitin in endocytosis and signaling. Science 315: 201-205, 2007.